Bayesian Limits on Primordial Isotropy Breaking

C. Armendariz-Picon and Larne Pekowsky

Physics Department, Syracuse University, Syracuse, New York 13244-1130, USA

(Received 21 July 2008; revised manuscript received 28 October 2008; published 20 January 2009)

It is often assumed that primordial perturbations are statistically isotropic, which implies, among other properties, that their power spectrum is invariant under rotations. In this article, we test this assumption by placing bounds on deviations from rotational invariance of the primordial spectrum. Using five-year Wilkinson Microwave Anisotropy Probe cosmic microwave anisotropy maps, we set limits on the overall norm and the amplitude of individual components of the primordial spectrum quadrupole and hexadecapole. We find that there is no significant evidence for primordial isotropy breaking, and constrain the relative contribution of the quadrupole and hexadecapole to be less than, respectively, 23% and 34% at 95% confidence level.

DOI: 10.1103/PhysRevLett.102.031301 PACS numbers: 98.80.Es

INTRODUCTION

Observations of the cosmic microwave background show that the early Universe contained tiny density perturbations, from which structures developed as the Universe expanded. In recent times, we have gained a wealth of information about these primordial perturbations. We have precisely measured their spectrum, and we have placed quite stringent limits on their properties [1]. Prompted by these advances, the nature of the primordial perturbations has entered the standard cosmological model, a set of a few parameters and assumptions that summarizes what we know about our Universe.

Even though the statistical isotropy of the CMB itself has been extensively investigated (see [2] and references therein) there is an assumption in the standard cosmological model that has not been subject to much observational or theoretical scrutiny: the statistical isotropy of the primordial perturbations themselves. Cosmological perturbations are statistically isotropic if their probability distribution functionals are invariant under rotations, which implies, in particular, that the power spectrum of statistically isotropic perturbations only depends on the magnitude of the wave vector, $\mathcal{P}(\mathbf{k}) = \mathcal{P}(k)$. Though some papers have analyzed the impact of statistically anisotropic perturbations on structure [3,4], while others have proposed mechanisms for their generation [5], to date no precise generic limits on the deviations from statistical isotropy of the primordial perturbations exist. In this Letter we set precise bounds, and thus verify one of the key ingredients in our understanding of the origin of structure.

STATISTICAL ANISOTROPY

In order to study deviations from statistical isotropy, we need to find an appropriate way to parametrize those deviations. Following [3], we expand the primordial power spectrum $\mathcal{P}_{\mathcal{R}}(\mathbf{k})$ in spherical harmonics,

$$\mathcal{P}_{\mathcal{R}}(\mathbf{k}) = \sqrt{4\pi}\sum_{\ell m}\mathcal{P}_{\ell m}(k)Y_{\ell m}(\hat{k}), \tag{1}$$

which in fact is the most general form the spectrum can take (we adhere to the normalization conventions of [1], which differ from those of [3]). For statistically isotropic perturbations only the "monopole" $\mathcal{P}_{00}$ is nonzero, whereas a nonvanishing $\mathcal{P}_{\ell m}$ for $\ell \neq 0$ is what characterizes statistically anisotropic Gaussian perturbations. We assume that the multipole components can be approximated by power laws,

$$\mathcal{P}_{\ell m}(k) = \mathcal{A}_{lm}\left(\frac{k}{2\times 10^{-3}\mathrm{Mpc}^{-1}}\right)^{n_s-1}, \tag{2}$$

with a common spectral index n_s. This is in fact what many of the models of primordial isotropy breaking predict in certain limits [5] (some of these models are unstable though [6]). In any case, because the range of scales we consider is relatively small, our results should also apply for mildly scale-dependent primordial spectrum multipoles, even if they do not share the same spectral index. Note that the $\mathcal{A}_{\ell m}$ are not completely arbitrary; they must vanish for odd values of ℓ [4].

We shall use cosmic microwave measurements to put constraints on the multipoles of the power spectrum. They are linked by the correlations between temperature multipoles that a statistically anisotropic power spectrum induces [3],

$$\langle a^*_{\ell_1 m_1} a_{\ell_2 m_2}\rangle = 4\pi(-i)^{\ell_2-\ell_1}\sum_{\ell m} D(\ell_1 m_1;\ell m;\ell_2 m_2) \times \int \frac{dk}{k}\Delta_{\ell 1}\Delta_{\ell 2}P_{\ell m}(k), \tag{3}$$

where the Δ_ℓ are the radiation transfer functions, and D is a product of Clebsch-Gordan coefficients. Note that Eq. (3) also applies for multipole expansions in real spherical harmonics, $Y^{\mathrm{real}}_{\ell m} \equiv [Y_{\ell|m|} + (-1)^m Y_{\ell|m|}]/\sqrt{2}$. For convenience we shall work here with the latter. In that case D is a linear combination of the complex D, determined by the unitary transformation that relates real and complex spherical harmonics.

BAYESIAN ANALYSIS

In this work we follow a Bayesian approach to inference, that is, we consider the posterior probability of the amplitudes $\mathcal{A}_{\ell m}$, given that we observe the temperature anisotropies $\mathbf{a}$,

$$P(\mathcal{A}_{\ell m}|\mathbf{a}) \propto L(\mathbf{a}|\mathcal{A}_{\ell m})P(\mathcal{A}_{\ell m}). \quad (4)$$

The function $L(\mathbf{a}|\mathcal{A}_{\ell m})$ is the likelihood, and $P(\mathcal{A}_{\ell m})$ is the prior. For notational convenience we gather the pair of multipole indices (ℓ, m) into a single index α, and we collect all the temperature anisotropies in a vector $\mathbf{a}$, with components a_α.

Because galactic contamination cannot be reliably removed from some regions of the sky, we are forced to deal with masked skies $\mathbf{c}$, from which those regions are excluded, $c(\hat{r}) = M(\hat{r}) \cdot T(\hat{r})$. The function M is the mask and T is the temperature signal. To proceed further, it is useful to have the counterpart of the last equation in multipole space, which can be readily shown to be

$$\mathbf{c} = M\mathbf{b},$$
$$\text{where } M_{\ell m,\ell_1 m_1} = \sum_{\ell_2 m_2} \frac{D(\ell m;\ell_1 m_1;\ell_2 m_2)}{\sqrt{4\pi}} M_{\ell_2 m_2}, \quad (5)$$

and the $b_{\ell m}$ are the spherical harmonic coefficients of the unmasked sky map.

But our troubles do not end here. In a real experiment, instruments have noise, and beams do not have infinite resolution. In addition, temperature maps are not provided as smooth functions over the sky, but rather, as pixelized functions over the sphere. Adding the instrument noise n to the cosmic microwave temperature, $T_{\text{observed}} = T_{\text{CMB}} + n$, and convolving the signal with, respectively, the instrument and pixel transfer functions W and H we arrive at the multipoles of the temperature map,

$$\mathbf{b} = HW\mathbf{a} + \mathbf{n}. \quad (6)$$

We use the Wilkinson Microwave Anisotropy Probe (WMAP) and HEALPIX beam transfer functions available at [7,8]. They are diagonal and m independent, and therefore do not take beam and pixel asymmetries into account.

The only problem left is to calculate how likely a particular temperature vector $\mathbf{c}$ is. Assuming that the temperature multipoles are Gaussian, inserting Eq. (6) into (5), and substituting into the analogue of Eq. (4) we obtain

$$P(\mathcal{A}_{\ell m}|\mathbf{c}) \propto \frac{1}{\det^{1/2} C} \exp(-\tfrac{1}{2}\mathbf{c} \cdot C^{-1}\mathbf{c}) P(\mathcal{A}_{\ell m}), \quad (7)$$

where C is the covariance matrix of the masked temperature multipoles,

$$C = (MHW)A(MHW)^T + MNM^T, \quad (8)$$

and A is the covariance matrix of the unmasked temperature anisotropies, Eq. (3). The matrix N is the pixel noise covariance matrix, with multipole components

$$N_{\ell_1 m_1,\ell_2 m_2} = \Delta a \sum_{\ell m} \frac{D(\ell_1 m_1;\ell_2 m_2;\ell m)}{\sqrt{4\pi}} N_{\ell m}, \quad (9)$$

where Δa is the area of each pixel in the temperature map, and $N_{\ell m}$ is the discrete spherical harmonic transform of the noise variance,

$$N_{\ell m} = \sum_i \Delta a N_i Y_{\ell m}(\hat{r}_i), \quad \text{where } \langle n_i n_j \rangle \equiv N_i \delta_{ij}. \quad (10)$$

The indices i and j run over all the pixels on the sphere.

DATA AND IMPLEMENTATION

Data

We analyze the five-year WMAP foreground-reduced $V2$ and $W1$ differential assembly temperature maps [1]. These are the maps with the lowest noise in the V and W frequency bands, which are the ones less exposed to foreground contamination. We do not consider combined frequency band maps here because they are averages of individual differential assemblies with direction-dependent weights. In general, for such averages the matrix W in Eq. (6) is not diagonal.

Because of computational limitations, it is not possible to analyze all the data in the maps. We restrict our analysis to masked temperate multipoles up to $\ell_{\text{max}} = 62$, and to a mask with bandwidth $\ell^M_{\text{max}} = 92$. Some of the masked multipoles have to be discarded however, as described below.

The noise power in the WMAP temperature maps is anisotropic. Though the monopole $\ell = 0$ is the dominant noise component, we also keep multipoles with $\ell = 4$, to make sure that anisotropies in the noise do not creep into our estimate of the primordial spectrum quadrupole. In any case, at $\ell_{\text{max}} + \ell^M_{\text{max}} = 154$, our errors are dominated by cosmic variance.

Mask

Starting from the WMAP 5-year temperature analysis/KQ85 mask (available at [7]) at HEALPIX resolution $N_{\text{side}} = 512$, we construct our analysis mask by sequentially following these steps: (i) Smooth with a Gaussian beam of FWHM = 600 arcmin, (ii) set pixels i with $M_i < 0.94$ to 0, and to 1 otherwise, (iii) smooth again with a Gaussian

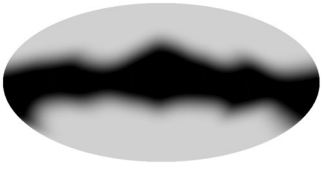

FIG. 1. Logarithm of the absolute value of our analysis mask. The absolute value of our mask in the innermost (black) regions of the galaxy is smaller than 10^{-9}. Our analysis mask covers 55% of the sky.

beam of FHWM = 300 arcmin, and, finally, (iv) set mask multipoles with $\ell > \ell^M_{\rm max} = 92$ to zero.

Figure 1 shows the logarithm of the absolute value of our mask. Because our mask is bandlimited, it cannot reproduce the original KQ85 mask. In particular, it does not cover the catalogued point sources, and it does not exactly vanish in the contaminated galactic region. To quantify the bias caused by an eventual galactic or point source contamination, we simulate 25 statistically isotropic random maps, and set the temperature of those pixels that would have been excluded by the original KQ85 mask to its value in the actual foreground-reduced $V2$ map. We then mask this artificial maps with our degraded mask and estimate the values of the amplitudes $\mathcal{A}_{\ell m}$ using our analysis pipeline. Their weighted means are collected in the last column of Table I. Of course, it is still possible for unresolved point sources to further contaminate our data, but this contamination is expected to be small at our resolution [9]. To make sure that our bounds do not depend on the mask, we repeat our analysis using a mask with $\ell^M_{\rm max} = 98$ and 60% sky coverage, and verify that this change does not significantly alter our results.

Markov Chain Monte Carlo

We sample the posterior probabilities in Eq. (7) with random-walk Monte Carlo Markov chains of 4×10^4 elements. We check for convergence of our chains using the spectral analysis method described in [10]. All our chains satisfy the convergence criteria described therein. We pick the starting point from previous runs, so no burn-in period is needed

Because the matrix M is ill conditioned, one cannot accurately calculate the inverse of C in the likelihood function (7) numerically. Instead, we determine the singular value decomposition of M^T, $M^T = U\Sigma V^T$, and consider the likelihood with $\mathbf{d} = V^T\mathbf{c}$ as data. Those modes d_α with $\Sigma_{\alpha\alpha} < \Sigma_{11}\sqrt{c(A)f}$ are removed from the analysis. The factor $f = 2.2 \times 10^{-16}$ is the floating number precision of our computer, and $c(A) \approx 10^3$ is the condition of the matrix A. The cut keeps 3523 out of 3965 modes.

We calculate the radiation transfer functions in Eq. (3) with a modified version of CMBEASY [11]. Since we fix the cosmological model, the transfer functions have to be computed only once.

RESULTS

We constrain the simplest deviations from statistical isotropy, namely, the quadrupole and hexadecapole of the primordial spectrum, $\mathcal{P}_{2m}$ and $\mathcal{P}_{4m}$, under the assumption (2). As discussed in [3], or just by symmetry, the expectation of scalar estimators of the temperature anisotropy multipoles C_ℓ only depends on $\mathcal{P}_{00}$. Hence, we can trust the cosmological parameters derived from fits to the angular spectrum C_ℓ even if primordial perturbations are statistically anisotropic. Here we use the ΛCDM parameters listed in the WMAP five-year cosmological parameter table at [7]. To check whether our limits depend on the assumed cosmological model, we repeat the analysis with the WMAP five-year ΛCDM + TENS parameter set [7]. Within statistical errors, our results do not change.

Rather than directly constraining the amplitude of the anisotropic components of the power spectrum, it is more convenient to study the posteriors of the monopole $\mathcal{A}_{00}$ and the ratios

$$\mathcal{R}_{\ell m} \equiv \frac{\mathcal{A}_{\ell m}}{\mathcal{A}_{00}}. \tag{11}$$

TABLE I. Sample mean and 95% credible intervals from the posterior distributions. In the last column we also list an estimate of the bias caused by galactic and point source contamination.

Parameter	$V2$	$W1$	$W1\|V2$	Bias
$\mathcal{A}_{00} \times 10^9$	2.43 ± 0.14	2.38 ± 0.13	2.40 ± 0.09	0.02
$\mathcal{R}_{2-2}$	-0.04 ± 0.09	-0.04 ± 0.09	-0.04 ± 0.06	-0.03
$\mathcal{R}_{2-1}$	-0.03 ± 0.08	-0.01 ± 0.09	-0.02 ± 0.06	-0.03
$\mathcal{R}_{20}$	0.06 ± 0.13	0.06 ± 0.13	0.05 ± 0.08	0.03
$\mathcal{R}_{21}$	0.08 ± 0.09	0.09 ± 0.09	0.09 ± 0.07	0.06
$\mathcal{R}_{22}$	-0.06 ± 0.10	-0.02 ± 0.10	-0.04 ± 0.07	-0.06
$\|\mathcal{R}_2\|$	<0.24	<0.23	<0.19	
$\mathcal{R}_{4-4}$	-0.11 ± 0.13	-0.16 ± 0.14	-0.14 ± 0.09	-0.05
$\mathcal{R}_{4-3}$	0.06 ± 0.12	0.05 ± 0.12	0.06 ± 0.08	0.06
$\mathcal{R}_{4-2}$	0.11 ± 0.11	0.12 ± 0.12	0.11 ± 0.09	0.05
$\mathcal{R}_{4-1}$	0.01 ± 0.12	-0.03 ± 0.13	-0.02 ± 0.09	0.01
$\mathcal{R}_{40}$	-0.01 ± 0.14	-0.01 ± 0.15	-0.00 ± 0.10	-0.03
$\mathcal{R}_{41}$	-0.05 ± 0.13	-0.07 ± 0.13	-0.05 ± 0.09	-0.03
$\mathcal{R}_{42}$	-0.11 ± 0.12	-0.12 ± 0.12	-0.11 ± 0.08	-0.05
$\mathcal{R}_{43}$	-0.01 ± 0.12	0.00 ± 0.12	-0.00 ± 0.07	-0.03
$\mathcal{R}_{44}$	0.08 ± 0.12	0.07 ± 0.12	0.08 ± 0.08	0.06
$\|\mathcal{R}_4\|$	<0.38	<0.41	<0.34	

In the analysis of the $V2$ and $W1$ maps we impose flat priors on all the parameters. The agreement of our constraints on $\mathcal{A}_{00}$ with those of the WMAP team provides a reassuring consistency check. We also analyze the $W1$ map using Gaussian priors derived from the results of our $V2$ analysis. This is what we label as $W1|V2$. Sample mean and 95% credible intervals in the $V2$, $W1$ and $W1|V2$ runs are listed in Table I, along with the bias caused by the imperfect mask. In order to quantify the overall magnitude of the multipoles, we use their norm

$$\|\mathcal{R}_\ell\| \equiv \sqrt{\sum_m \mathcal{R}^2_{\ell m}}, \tag{12}$$

which is invariant under rotations.

We might also extend our analysis to assess whether statistically isotropic perturbations are a better model for the data. Since we cannot compute the Bayesian evidence within our approach, we determine instead three nonexclusively Bayesian measures that have been widely used in the literature: the effective chi squared, $\chi^2_{\rm eff} \equiv -2\log L_{\rm max}$, the Akaike information criterion (AIC) and the Bayes information criterion (BIC) (see, for instance, [12]). Their differences under the assumptions of a nonvanishing and vanishing quadrupole are listed in Table II.

CONCLUSIONS

Inspection of Table I quickly reveals that the amplitude of the anisotropic components is consistent with statistical isotropy. In particular, we exclude the relative contribution of the quadrupole to the total power to be less than 24%, and that of the hexadecapole to be less than 34% at the 95% confidence level. The results in Table II also imply that there is no evidence for primordial statistical anisotropy. Although a nonzero primordial quadrupole significantly increases the likelihood, the information criteria that penalize the introduction of additional parameters strongly favor isotropy.

Because any deviation from statistical isotropy can be cast as in Eq. (1), the limits that we have found are quite generic, and can thus be directly applied to any of the models for the generation of (adiabatic) statistically anisotropic perturbations discussed in the literature [5] that satisfy condition (2). We have not studied how our bounds constrain the parameters of these models, but it should be straightforward to do so. On the other hand, our null results confirm again the predictions of the simplest inflationary models.

TABLE II. Comparison between fits to the data with a nonvanishing and a vanishing quadrupole, $\Delta X = X_{\rm ani} - X_{\rm iso}$. The inclusion of a quadrupole and hexadecapole in the primordial power spectrum introduces 14 additional parameters.

Criterion	$\Delta\chi^2_{\rm eff}$	ΔAIC	ΔBIC
$V2$	-17.2	10.8	97.1
$W1$	-17.0	11.0	97.3

The study of the statistical isotropy of the primordial perturbations is still in its infancy, and our analysis is just a first step toward more precise measurements of the primordial spectrum. With more data, improved analysis techniques, and better control of systematics, it should be possible in principle to obtain much tighter constraints [4].

We acknowledge the use of the Legacy Archive for Microwave Background Data Analysis (LAMBDA), and thank an anonymous referee for useful suggestions. Support for LAMBDA is provided by the NASA Office of Space Science. Some of the results in this Letter have been derived using the HEALPIX [13] package. The work of C. A. P. is supported in part by the National Science Foundation under Grant No. PHY-0604760. Shortly before submission of this manuscript, an article with significant overlap with the work presented here appeared on the arXiv [14]. The signal reported in the latter corresponds to a quadrupole component of order $\|\mathcal{R}_2\| \approx 0.1$, and is thus compatible with our limits.

[1] E. Komatsu *et al.* (WMAP Collaboration), arXiv:0803.0547.
[2] T. Souradeep, A. Hajian, and S. Basak, New Astron. Rev. **50**, 889 (2006).
[3] C. Armendariz-Picon, J. Cosmol. Astropart. Phys. 03 (2006) 002.
[4] A. R. Pullen and M. Kamionkowski, Phys. Rev. D **76**, 103529 (2007); S. Ando and M. Kamionkowski, Phys. Rev. Lett. **100**, 071301 (2008).
[5] L. Ackerman, S. M. Carroll, and M. B. Wise, Phys. Rev. D **75**, 083502 (2007); C. Armendariz-Picon, J. Cosmol. Astropart. Phys. 09 (2007) 014; T. S. Pereira, C. Pitrou, and J. P. Uzan, J. Cosmol. Astropart. Phys. 09 (2007) 006; C. Pitrou, T. S. Pereira, and J. P. Uzan, J. Cosmol. Astropart. Phys. 04 (2008) 004; A. E. Gumrukcuoglu, C. R. Contaldi, and M. Peloso, J. Cosmol. Astropart. Phys. 11 (2007) 005; E. Akofor, A. P. Balachandran, S. G. Jo, A. Joseph, and B. A. Qureshi, J. High Energy Phys. 05 (2008) 092; S. Yokoyama and J. Soda, J. Cosmol. Astropart. Phys. 08 (2008) 005; A. L. Erickcek, M. Kamionkowski, and S. M. Carroll, Phys. Rev. D **78**, 123520 (2008).
[6] B. Himmetoglu, C. R. Contaldi, and M. Peloso, arXiv:0809.2779.
[7] http://lambda.gsfc.nasa.gov
[8] http://healpix.jpl.nasa.gov
[9] E. Pierpaoli, Astrophys. J. **589**, 58 (2003).
[10] J. Dunkley, M. Bucher, P. G. Ferreira, K. Moodley, and C. Skordis, Mon. Not. R. Astron. Soc. **356**, 925 (2005).
[11] M. Doran, J. Cosmol. Astropart. Phys. 10 (2005) 011.
[12] A. R. Liddle, Mon. Not. R. Astron. Soc. Lett. **377**, L74 (2007).
[13] K. M. Gorski, E. Hivon, A. J. Banday, B. D. Wandelt, F. K. Hansen, M. Reinecke, and M. Bartelman, Astrophys. J. **622**, 759 (2005).
[14] N. E. Groeneboom and H. K. Eriksen, arXiv:0807.2242.